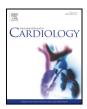
ARTICLE IN PRESS

International Journal of Cardiology xxx (2018) xxx-xxx



Contents lists available at ScienceDirect

International Journal of Cardiology



journal homepage: www.elsevier.com/locate/ijcard

Implications of the local hemodynamic forces on the formation and destabilization of neoatherosclerotic lesions

Ryo Torii ^a, Rodrigue Stettler ^b, Lorenz Räber ^c, Yao-Jun Zhang ^{d, j}, Antonis Karanasos ^e, Jouke Dijkstra ^f, Kush Patel ^b, Tom Crake ^b, Steve Hamshere ^b, Hector M. Garcia-Garcia ^e, Erhan Tenekecioglu ^e, Muhiddin Ozkor ^b, Andreas Baumbach ^{b,g}, Stephan Windecker ^c, Patrick W. Serruys ^{e,h}, Evelyn Regar ^k, Anthony Mathur ^{b,g}, Christos V. Bourantas ^{b,g,i,*}

^a Department of Mechanical Engineering, University College London, London, United Kingdom

^b Barts Heart Centre, Barts Health NHS, London, United Kingdom

^c Bern University Hospital, Bern, Switzerland

^d Xuzhou Third People's Hospital, Jiangsu University, Xuzhou, China

^e Thoraxcenter, Erasmus Medical Centre, Rotterdam, the Netherlands

^f Leiden University Medical Centre, Leiden, the Netherlands

^g Queen Mary University London, London, United Kingdom

^h Faculty of Medicine, National Heart & Lung Institute, Imperial College London, United Kingdom

ⁱ Institute of Cardiovascular Sciences, University College London, London, United Kingdom

^j Nanjing First Hospital, Nanjing Medical University, Nanjing, China

^k Department of Cardiovascular Surgery, University Hospital Zürich, Zürich, Switzerland

ARTICLE INFO

Article history: Received 30 March 2018 Received in revised form 18 May 2018 Accepted 18 June 2018 Available online xxxx

Keywords: Neoatherosclerosis Endothelial shear stress Optical coherence tomography

ABSTRACT

Objective: To examine the implications of endothelial shear stress (ESS) distribution in the formation of neoatherosclerotic lesions.

Methods: Thirty six patients with neoatherosclerotic lesions on optical coherence tomography (OCT) were included in this study. The OCT data were used to reconstruct coronary anatomy. Blood flow simulation was performed in the models reconstructed from the stent borders which it was assumed that represented the lumen surface at baseline, immediate after stent implantation, and the estimated ESS was associated with the neointima burden, neoatherosclerotic burden and neointima characteristics. In segments with neointima rupture blood flow simulation was also performed in the model representing the lumen surface before rupture and the ESS was estimated at the ruptured site.

Results: An inverse association was noted between baseline ESS and the incidence and the burden of neoatherosclerotic ($\beta = -0.60$, P < 0.001, and $\beta = -4.05$, P < 0.001, respectively) and lipid-rich neoatherosclerotic tissue ($\beta = -0.54$, P < 0.001, and $\beta = -3.60$, P < 0.001, respectively). Segments exposed to low ESS (<1 Pa) were more likely to exhibit macrophages accumulation (28.2% vs 10.9%, P < 0.001), thrombus (11.0% vs 2.6%, P < 0.001) and evidence of neointima discontinuities (8.1% vs 0.9%, P < 0.001) compared to those exposed to normal or high ESS. In segments with neointima rupture the ESS was high at the rupture site compared to the average ESS over the culprit lesion (4.00 ± 3.65 Pa vs 3.14 ± 2.90 Pa, P < 0.001).

Conclusions: Local EES is associated with neoatherosclerotic lesion characteristics, which suggests involvement of ESS in the formation of vulnerable plaques in stented segments.

© 2018 Elsevier B.V. All rights reserved.

1. Introduction

Local hemodynamic forces and in particular endothelial shear stress (ESS) appear to regulate atherosclerotic evolution in native coronary arteries. Experimental studies have shed light onto the

https://doi.org/10.1016/j.ijcard.2018.06.065 0167-5273/© 2018 Elsevier B.V. All rights reserved. mechanotransduction processes that regulate plaque formation and provided robust evidence that ESS is involved in the formation of high-risk vulnerable lesions, while clinical studies demonstrated that ESS is also a predictor of lesions that are likely to progress and cause cardiovascular events [1].

In stented segments short-term follow-up intravascular imaging studies have shown that ESS determines neointima proliferation in bare metal stents (BMS) and bioresorbable scaffolds, while in drug eluting stents (DES) this effect – at least at short-term – is inhibited by the

Please cite this article as: R. Torii, et al., Implications of the local hemodynamic forces on the formation and destabilization of neoatherosclerotic lesions, Int J Cardiol (2018), https://doi.org/10.1016/j.ijcard.2018.06.065

^{*} Corresponding author at: Barts Heart Centre, 1st St Martin's le Grand, London EC1A 7BE, United Kingdom.

E-mail address: Christos.Bourantas@bartshealth.nhs.uk (C.V. Bourantas).

2

ARTICLE IN PRESS

R. Torii et al. / International Journal of Cardiology xxx (2018) xxx-xxx

antiproliferative drug [2, 3]. However, to date there are no data about the long-term implications of the local hemodynamic forces on neointima growth and about their role in the formation of neoatherosclerotic lesions. The objectives of this study are: 1) to examine the role of the ESS on the formation of neoatherosclerotic plaques and 2) its implications on neoatherosclerotic plaque destabilization.

2. Methods

2.1. Patient population

This is a retrospective analysis of optical coherence tomographic (OCT) data acquired from patients with neoatherosclerotic lesions that underwent OCT imaging for suspected stent failure. Five experts (RS, LR, AK, YZ and CB) reviewed the OCT databases in four University Hospitals (St Bartholomew Hospital Barts Health NHS Trust, Bern University Hospital, Nanjing First Hospital and Thoraxcentre Erasmus MC) and identified consecutive patients with neoatherosclerotic lesions that had OCT imaging for suspected stent failure. All the recruited patients had complete assessment of the stented segment with Fourier Domain OCT before balloon pre-dilation. OCT examinations with poor imaging quality, and extensive thrombus or extensive neointima disruptions that did not allow accurate delineation of the lumen were excluded from the analysis. In addition, segments implanted with different stent types (i.e., with BMS and DES or with a 1st and 2nd generation DES), segments with extensive stent overlapping (>5 mm) and those where the stent border could not be assessed for a circumference of >180° in a length >0.8 mm were excluded from the analysis of the effect of ESS on neoatherosclerotic lesion formation. Segments that exhibited neointima rupture - even those with extensive overlapping and those where the stent border was not visible in the entire pullback - were used to examine the implications of ESS on neointima destabilization (Supplementary Fig. 1).

Sirolimus (Cypher, Cordis, Miami Lakes, FL) and Paclitaxel (Taxus, Boston Scientific, Natick, MA) eluting stents were classified as 1st generation DES, while Zotarolimus (Endeavor Sprint or Resolute, Medtronic, Santa Rosa, CA), Biolimus (BioMatrix, Biosensors Inc., Singapore) and Everolimus (Xience, Abbott Vascular, Abbott Park, IL) as 2nd generation DES. Segments implanted with a stent of unknown type were also excluded from the analysis.

2.2. Optical coherence tomography - data acquisition

OCT imaging was performed with a C7XR, an OPTIS™ (St-Jude Medical, Westford, MA, USA) or a Lunawave (Terumo Corp, Tokyo Japan) Fourier Domain system. In segments with increased thrombus burden, thrombus aspiration was undertaken before OCT imaging. Pull-back was performed with the use of an automated pull-back device at a constant speed (range: 18–40 mm/s) during continuous injection of contrast medium (frame rates: 180 fr/s for the OPTIS, 100 fr/s for the C7XR and 160 fr/s for the Lunawave system).

2.3. Segmentation of optical coherence tomographic data

OCT imaging analysis was performed offline using proprietary software (QCM-CMS Medis Medical Imaging System, Leiden, The Netherlands). The stented segments were identified and the most proximal and distal side branches that were visible in both OCT and X-ray angiographic images were detected and used to define the segment of interest. The OCT frames portraying this segment were analyzed at 0.4 mm interval (0.375 mm for the Lunawave system) by two independent analysts (RS and CVB) blinded to stent type and patients' characteristics. The lumen borders in the non-stented segment of interest and the lumen and stent borders – defined by a curve connecting the hyper-intense signal of the metallic struts – in the stented segment were detected. Neointima was defined as the effect of ESS on plaque rupture in frames with neointima discontinuities an additional border was drawn that connected the edges of the ruptured fibrous cap and represented the lumen surface before neointima rupture (Supplementary File) [4].

Neoatherosclerosis was defined as neointima with lipid and/or calcific tissue. In frames with neoatherosclerotic lesions the lipid and calcific tissue borders were detected and their areas were estimated (Supplementary File). In addition, the minimum cap thickness was estimated and used to classify the neoatherosclerotic plaques as thin (TCFA, minimum cap thickness \geq 65 µm). Finally, the presence of thrombus, macrophage accumulations, neovesels and cholesterol crystals were detected (Supplementary File).

2.4. Reconstruction of coronary anatomy

A well established and validated methodology was used to reconstruct the segments of interest [5]. In brief, this approach involves the extraction of the luminal centreline from 2 angiographic projections, the placement of the OCT borders onto the luminal centreline and the estimation of the absolute orientation of the OCT borders using established algorithms that take into account the origin of side branches identified in both OCT and angiographic projections. The OCT data acquired at the time of the event was used to reconstruct two models for each studied vessel: the first was reconstructed from the lumen borders in the non-stented segment and the stent borders in the stented segment, and it was assumed to represent the lumen surface at baseline immediately after stent implantation (baseline model), and the second from the lumen borders both in the stented

and non-stented segments and corresponded to the lumen geometry at follow-up (follow-up model). In addition, in segments with neointima discontinuities, a third model was reconstructed from the lumen borders before neointima rupture and this represented the lumen geometry before the cardiovascular event (pre-rupture model). More specifically, similar to previous studies investigating the effect of ESS on plaque rupture, in frames portraying neointima rupture we approximated the lumen border before rupture by drawing an arc that connected the edges of the ruptured fibrous cap [4]. Blood flow simulation was performed at the baseline and the pre-rupture models and the ESS was estimated (Supplementary File).

2.5. Data analysis

Analysis was restricted in the stented segment. Each stented segment in each reconstructed artery was divided into consecutive 1.5-mm sub-segments and for each subsegment the minimum predominant ESS was estimated at the baseline model as previously described [2]. In addition, for each 1.5 mm segment the mean lumen area, the mean stent area, the mean neointima area and burden (defined as: $100 \times$ neointima area / stent area), the mean lipid tissue and calcific tissue area and burden and the minimum cap thickness over lipid tissue – defined as the minimum thickness of the fibrous cap in the 1.5 mm sub-segment – were estimated.

In stented segments with neointima discontinuities, neointima ruptures – indicated by the presence of a cavity or a flap on OCT – were identified. We define as a ruptured lesion a segment that had neointima rupture and exhibited a maximum stenosis (throat), two shoulders and an upstream and downstream segment. The upstream and downstream segments were characterised as segments exhibiting progressive narrowing from their distal end towards the throat. The most proximal and distal to the throat OCT frames that had a mean neointima thickness >0.5 mm were assumed that corresponded to the proximal and distal end of the ruptured lesion [4]. To examine the effect of ESS on plaque rupture we performed blood flow simulation in the pre-rupture model and estimated the local ESS – not the predominant – at the rupture site and compared them with the average ESS at the ruptured lesion and the average luminal ESS at the remaining stented segment [4, 6].

2.6. Statistical analysis

Continuous variables are reported as mean \pm standard deviation when they are normally distributed and median and interquartile range (IQR) when they are not normally distributed. Categorical values are presented as absolute value and percentage. Anova and Kruskal-Wallis test – depending on variables' distribution – were used for independent group comparison of continues variables and chi-square test was used to compare categorical variables. In order to examine associations between the minimum predominant ESS and OCT-derived variables in 1.5 mm sub-segments, linear-mixed effect models were used: stent type and stent cross-sectional area were considered as fixed factors, and each individual patient was considered as random effect to account for intra-individual dependency. For the binomial dependent variables such as presence of neoatherosclerosis in a segment, generalised mixed–effect models (logistic regression) were used. A P-value < 0.05 was considered statistical significant. Analysis was performed with the SPSS 20 (SPSS Inc., Chicago, IL) and the open-source R (version 3.3.0) statistical packages.

3. Results

3.1. Patients' characteristics

From November 2009 till June 2016, 43 patients were deemed suitable for inclusion in the study. After reviewing the data, 36 patients (36 segments: 11 implanted with a BMS, 12 with a 1st generation DES and 13 with a 2nd generation DES) were included in the study, of which 34 in the analysis that investigated the association between neoatherosclerosis and ESS distribution (Supplementary Fig. 1). Two patients were excluded because of lack of optimal angiographic projections that are required for the reconstruction of coronary anatomy, 1 because of extensive overlapping, 1 because of no neoatherosclerotic lesion, 1 because of the fact that the stent type was not known and 2 because it was not possible to accurately delineate the stent borders.

From the 36 patients that were included in the analysis, 30 had an event because of a neoatherosclerotic lesion (10 exhibited neointima rupture and 20 significant restenosis because of a neoatherosclerotic plaque), 2 had an event because of restenosis attributed to excessive neointima proliferation and 4 did not have significant in stent restenosis.

The effect of the local hemodynamic forces on neointima rupture was assessed in 10 segments; in 8 segments that were included in neoatherosclerosis analysis and in 2 segments, implanted with a 2nd generation DES, that were excluded from the neoatherosclerosis analysis because of extensive stent overlapping or increased lipid-rich neointima that did not allow visualization of the stent border in a segment

Please cite this article as: R. Torii, et al., Implications of the local hemodynamic forces on the formation and destabilization of neoatherosclerotic lesions, Int [Cardiol (2018), https://doi.org/10.1016/j.ijcard.2018.06.065

Download English Version:

https://daneshyari.com/en/article/11014983

Download Persian Version:

https://daneshyari.com/article/11014983

Daneshyari.com